Int. J. Electrochem. Sci., 17 **(2022)** Article Number: 220848, doi: 10.20964/2022.08.50

International Journal of
ELECTROCHEMICAL
SCIENCE
www.electrochemsci.org

Chitosan-Clay Nanocomposite as a Green Corrosion Inhibitor for Mild Steel in Hydrochloric Acid Solution

Waad M. Alotaibi[1,*], *Saedah R. Al-Mhyawi*[2], *Soha M. Albukhari*[3]

[1] King Abdulaziz City for Science and Technology, Riyadh 11442, Saudi Arabia.
[2] Chemistry Department, Faculty of Science, University of Jeddah, Jeddah, Saudi Arabia,
[3] Chemistry Department, Faculty of Science, King Abdulaziz University, Jeddah, Saudi Arabia
[*]E-mail: waad111777@gmail.com

Received: 14 March 2022 / *Accepted:* 30 May 2022 / *Published:* 4 July 2022

In this study, chitosan-montmorillonite nanocomposites were prepared by dispersing inorganic nanolayers of clay in an organic polymer matrix via direct melt intercalation. Characterizations were performed using different methods, i.e., FTIR, NMR, SEM and AFM. This nanocomposite was used as a corrosion inhibitor. The anti-corrosion behavior of the nanocomposite on mild steel was investigated by electrochemical measurements such as electrochemical impedance spectroscopy (EIS) and potentiodynamic polarization (PDP) in hydrochloric solution acid. The results indicated that nanocomposite inhibits mild steel corrosion in 1.0 M HCl. The PDP results showed that chitosan-montmorillonite nanocomposites act as mixed-type inhibitors.

Keywords: Nanocomposites; Clay; Chitosan; Corrosion

1. INTRODUCTION

Recently, polymer-clay nanocomposites have become the field of active research in many applications, such as fire retardants, oxygen barriers, thermal stability, corrosion inhibitors, etc. [1]. This nanocomposite improves the thermal, mechanical and gas barrier properties at a low clay content of approximately 10 wt % [2]. This nanoclay (nanoscale silicates) with high porosity can influence the polymeric matrix to form nanocomposites with desired properties. In this study, inorganic platelets (nanoclay) are embedded in the polymer matrix to form nanocomposites, which are used as corrosion inhibitors. The resulting green corrosion inhibitor is desired because first, it provides metal protection by physically blocking the metal surface from the corrosion environment. Second, it has low cost, low toxicity and good sustainability. Third, nanoclay avoids the environmental unfriendliness of inorganic and organic corrosion inhibitors Smectite clays, for example, montmorillonite (MMT), is the most

widely used layered silicates for the preparation of polymer-clay nanocomposites because they have a high aspect ratio (10-1000) and a huge cationic exchange capacity [3]. It is a typical 2:1 layered structure. Montmorillonite has a sandwich-type structure with one octahedral aluminum. The chemical composition of the montmorillonite Clay is $(Na, Ca)_{0.33}$ $(Al, Mg)_2(Si_4O_{10})$ $(OH)_2 \cdot nH_2O$ [4]. MMT has high ion exchange capacity, adsorption, affordability, and storage capacity, and is used in many fields such as chemical, environmental, food, pharmaceutical, energy and other fields. [5]. There are several different agents used to modify the MMT clay like a cationic surfactant, an anionic surfactant or a silane coupling agent to make them compatible with polymer [6]. Modified MMT clay is used for making eco-friendly polymer clay nanocomposites with improved physical and mechanical properties [7].

Aminosilane coupling agents in Figure (1) act in the interphase region, the area between an inorganic substrate such as glass, minerals and metals and an organic substrate like polymers [8]. N-aminoethyl-3-aminopropyl-trimethoxysilane (aminosilane) was used for the cation exchange of mineral ions in the structure of montmorillonite, as a result of which is in a hydrophobic clay mineral and a larger surface area for the interlayer [9].

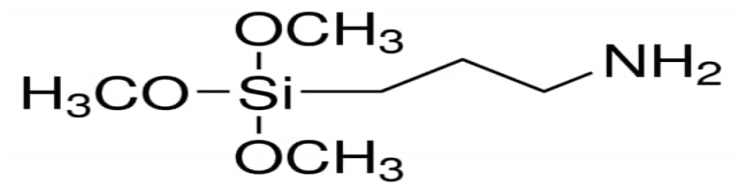

Figure 1. Structure of n-aminoethyl-3-aminopropyltrimethoxysilane (aminosilane).

Chitosan is one of the most exciting biopolymers obtained from natural sources [10]. It is known as deacetylated chitin [11]. There are various chemical properties of chitosan, including its inexpensive, nontoxic and hydrophilic character [12]. Additionally, it has antibacterial, biocompatible, and biodegradable properties, making it widely applicable in biomedical fields [13]. Chitosan blending with montmorillonite clay is used to make composite films, sensors, absorbent materials, enzyme immobilization supports, and nanocomposites [14].

In the present work, we prepared chitosan- montmorillonite nanocomposite as a green corrosion inhibitor for mild steel in hydrochloric acid solution.

2. EXPERIMENTAL

2.1. Materials

Sodium montmorillonite (Cloisite Na+, Southern Clay Products) with a cation-exchange capacity (CEC) of 92 mequiv/100 g, platelets average size (110 nm) as described by the manufacturer (Sigma-Aldrich).

N-aminoethyl-3-aminopropyl-trimethoxysilane (aminosilane) 97% purchased from Sigma-Aldrich. Chitosan (Mw 190,000–375,000), viscosity (200 cps), degree of deacetylation (DD 75–85%) (Sigma-Aldrich) and Methanol (commercial).

2.2. Specimens and Surface Pretreatment

The mild steel sample was kindly provided by the SABIC Company. The chemical structure of the specimen of mild steel used is presented in Table (1). The specimen was cut in the form of a sheet, 3 cm long, 1.5 cm wide and 3 mm thick. Before exposure, the specimen was polished using 60,120,150,400,800 and 1000 emery paper grades. After this process, the specimen was washed with double-distilled water and finally degreased with acetone. All experiments were carried out in freshly prepared solutions.

Table 1. Composition of mild steel specimen.

Element	C	Si	Mn	P	S	N	Cu	Ni	Fe
Percent%	0.050	0.01	0.197	0.0079	0.0074	0.0026	0.0145	0.0191	Reminder

2.3. Solutions

Hydrochloric acid was used to prepare the aggressive solution (1.0 M) by dilution of analytical grade with distilled water. The concentrations of chitosan-montmorillonite nanocomposite (0.1-1.5) g/L were prepared by adding the nanocomposite inhibitor to the test solutions. The volume for the experiment of the electrochemical measurements was 100 mL in test solutions

2.4. Preparation of (Chitosan-MMT) Nanocomposite

In this study, we used the dispersion method to prepare (chitosan-MMT) nanocomposite. The preparation method as shown in Figure 2 is:

□□A 5 wt% clay disperse in 100 ml of methanol under stirring for 2h.

□□Suspension 1: Add 10wt% aminosilane with respect to nanoclay wt (5% aq / 10% aq) to form (nanoclay-sailan) dispersion solution (stir 2h, ultrasonicate 30 min).

□□Suspension 2: Chitosan (5% aq) disperse in methanol (stir 2h, ultrasonicate 30 min).

Blend suspension 1 and 2, heat to 60 ^{o}C 1h, continue stirring for 24h, and then (ultrasonicate 30 min).

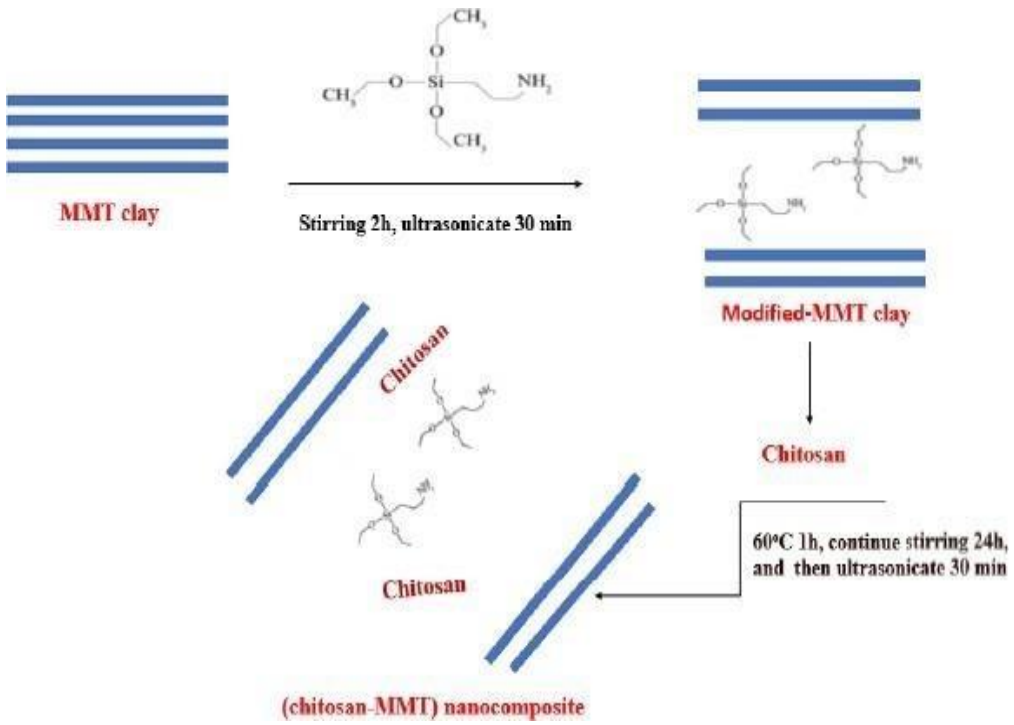

Figure 2. Schematic diagram of chitosan-montmorillonite nanocomposite synthesis.

2.5. Characterization

2.5.1. Fourier Transform Infrared Spectroscopy (FTIR)

The IR spectrum was studied on an FTIR Total Reflectance (ATR) Brucker Tensor II spectrometer. The obtained spectra were obtained over a range of 4000 to 600 cm^{-1} with a spectral resolution of 4 cm^{-1} using OPUS Bruker software.

2.5.2. Nuclear Magnetic Resonance (NMR)

$^{1}H/^{13}C$-NMR spectra were obtained with a Bruker AV-400 MHZ multinuclear probe spectrometer. Chemical shifts are listed according to the δ scale in ppm and refer to the nondeuterated part of the used solvent deuterated chloroform [($CDCl_3$)] at 7.26 ppm for ^{1}H NMR and 77 ppm for ^{13}C NMR.

2.5.3. Surface analysis

The sample morphology was examined by field emission scanning electron microscopy (FEG-SEM, Quanta FEG450, FEI, the Netherlands) and AFM images were studied using a UHV VT AFM XA (OMICRON GMBH) in contact mode Si cantilevers at room temperature.

3. RESULTS AND DISCUSSION

3.1. Characterization of the chitosan-montmorillonite nanocomposites

The FTIR spectra of MMT clay, chitosan and chitosan-MMT clay are shown in Figure (3), in which MMT showed a band at 2450 cm^{-1} corresponding to the vibration of the C– H bond. The peak at 1040 cm^{-1} is due to Si–O stretching. We observed at 916 and 840 cm^{-1}, respectively, the bands of the Al-O-Si and Si-O-Si bending vibrations. The presence of a broad peak at 3426 cm^{-1} in the spectrum of chitosan is attributed to hydroxyl groups. The absorption bands at approximately 2921 and 2877 cm^{-1} attributed to C-H symmetric and asymmetric stretching, respectively, while peaks appearing at 1646 cm^{-1} and 1383 cm^{-1} correspond to the stretching vibrational frequencies of amide Iand amide III in chitosan molecules, respectively. The bands at 1066 and 1028 cm^{-1} correspond to C-O stretching [15]. Nanocomposite stretching vibrations are those related to chitosan and the montmorillonite spectra. The band of Si–O groups of clay related with amino groups at 1021–1080 cm^{-1} by hydrogen bonding interactions between NH^{3+} and the negatively charged sites of clay.

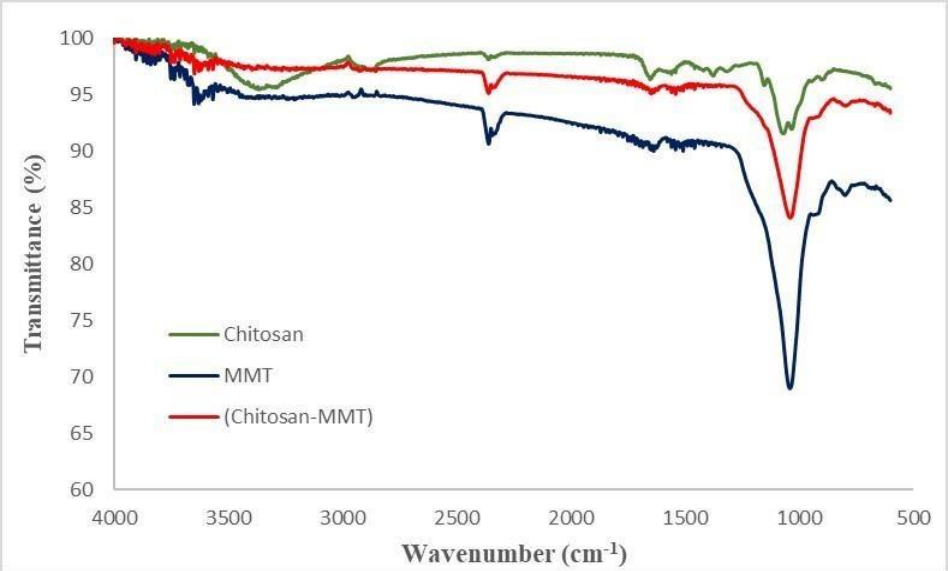

Figure 3. FTIR spectra of chitosan-montmorillonite nanocomposites.

Figure (4) displays the ^{1}H NMR spectrum of chitosan $C_{56}H_{103}N_9O_{39}$ which shows signals at δ 0.8022, 1.5110 and 7.1978 due to the carbons of the N-acetyl glucosamine rings and the acetyl group.

The ^{13}C NMR spectrum of aminosilane in Figure (5) shows signals at δ 29.7227 ppm due to the carbons of the acetyl group.

In addition, the expected chemical shifts in the regions 76.8888, 77.0393, 77.1877 and 77.2414 due to the carbons in the N-glucosamine ring are expected to be affected by this interaction with the clay

as a "bridge model" where several chitosan functional groups (amine and hydroxyl) are bound with metal ions from the same backbone or different ones via inter or intramolecular complexation [16].

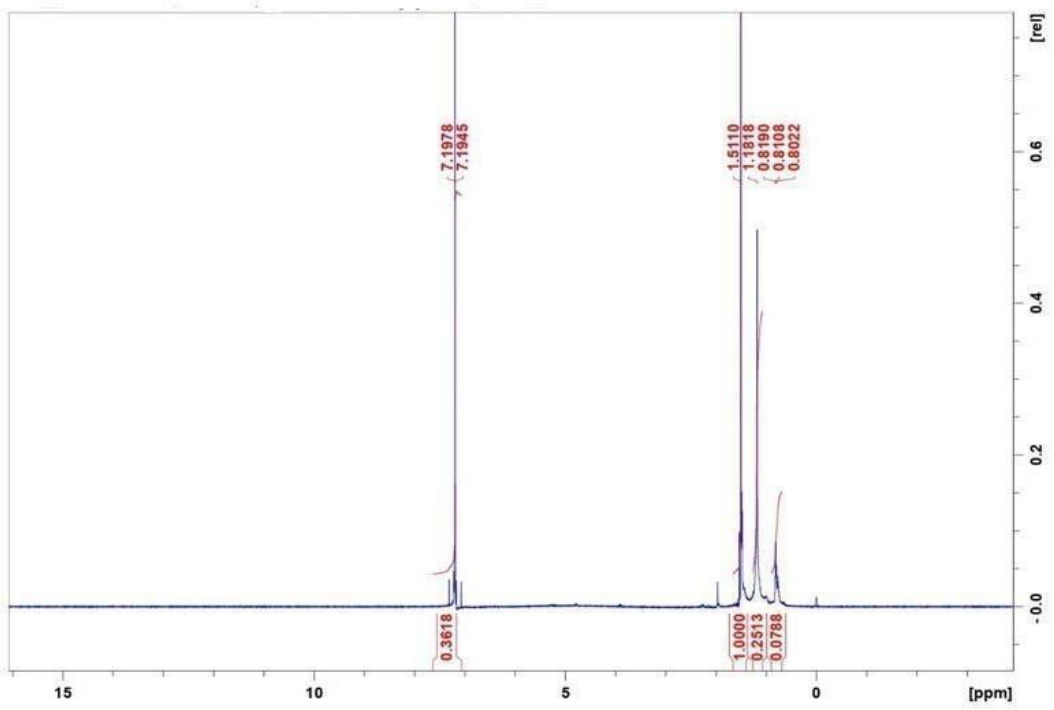

Figure 4. [1]H NMR of chitosan-montmorillonite nanocomposites.

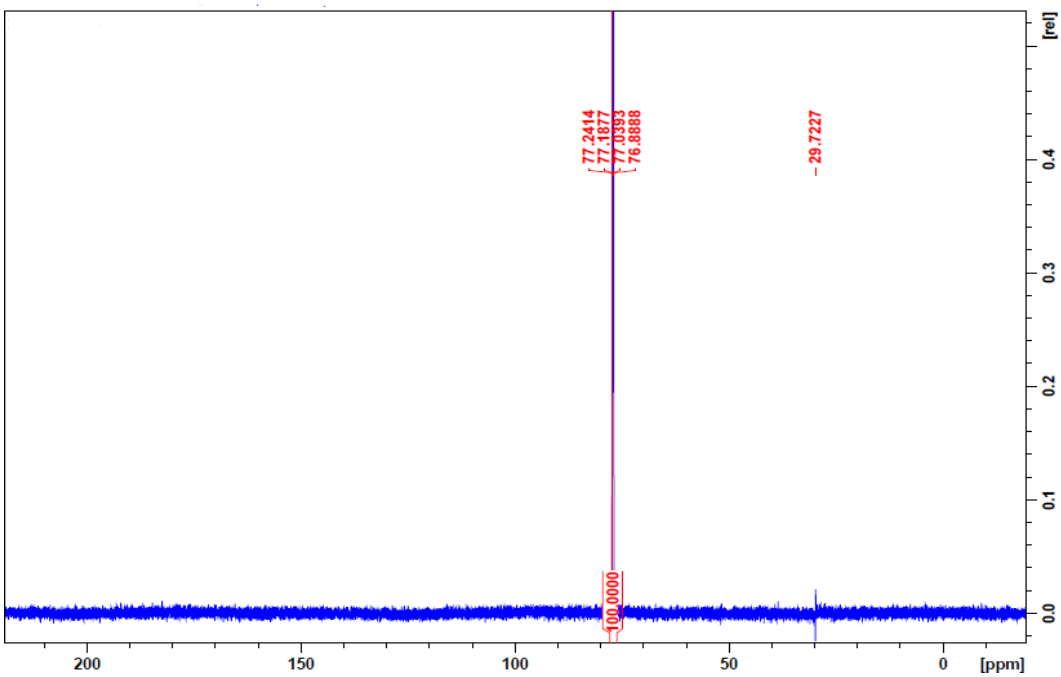

Figure 5. [13]C NMR of chitosan-montmorillonite nanocomposites.

3.2. Corrosion studied

The effect of chitosan-montmorillonite nanocomposites on the corrosion of mild steel in 1.0 M HCl was studied under different conditions using electrochemical measurements (EIS, PDP).

3.2.1 Impedance and potentiodynamic polarization study

Figure (6) shows the Nyquist diagrams for mild steel in 1.0 M HCl in the absence and presence of different concentrations (0.1-1.5 g/L) of chitosan-montmorillonite nanocomposite at 30 °C.

The impedance plots gave a semicircle-type appearance to indicating the corrosion of mild steel is mainly controlled by a charge transfer process and that the presence of the chitosan-montmorillonite nanocomposite in solution does not alter the mechanism of dissolution of mild steel, as in 1.0 M HCl solution. The diameter of the semicircle increases with the increasing concentration of the nanocomposite, at a maximum value of 74.08% in 1.0 M HCl, indicating an increase in the corrosion resistance of the mild steel metal.

As seen in Table (2), the presence of inhibitor enhances the value of the charge-transfer resistance (R_{ct}) in 1.0 M HCl. The values of R_{ct} increase with increasing inhibitor concentration. Additionally, the values of double-layer capacitance (C_{dl}) are decreased in the presence of chitosan- montmorillonite nanocomposites. The inhibition efficiency *(% IE*)is calculated using Equation (1).

$$\%IE = \frac{R_{ct(inh)} - R_{ct}}{R_{ct(inh)}} \; x\,100 \qquad (1)$$

Where $R_{ct_{(inh)}}$ and R_{ct} are the charge-transfer resistances obtained under the condition of inhibited and uninhibited solution, respectively [17].

Figure (7) shows the potentiodynamic polarization (PDP) curves for mild steel in 1.0 M HCl in the absence and presence of different concentrations (0.1-1.5 g/L) of the chitosan-montmorillonite nanocomposite. The electrochemical parameters corrosion potential (E_{corr}), corrosion current density (I_{corr}), anodic and cathodic Tafel slopes (β_a and β_c) and (%*IE*) are recorded in Table (3). Equations (2) and (3) respectively, using to calculate the inhibition efficiency (%IE) of the compound and surface coverage on the metal surface by the inhibitor (θ).

$$\%IE = \frac{i_{corr} - i_{corr_{(inh)}}}{i_{corr}} \; x\,100 \qquad (2)$$

Where i_{corr} and $i_{corr_{(inh)}}$ are corrosion current density without and with chitosan-montmorillonite nanocomposite [18].

$$\theta = \frac{IE\%}{100} \qquad (3)$$

The chitosan-montmorillonite nanocomposites affect both the anodic and cathodic curves of mild steel, the inhibitor acted as a mixed-type inhibitor. The corrosion current density decreases with increasing inhibitor concentration, which leads to an increase in inhibition efficiency.

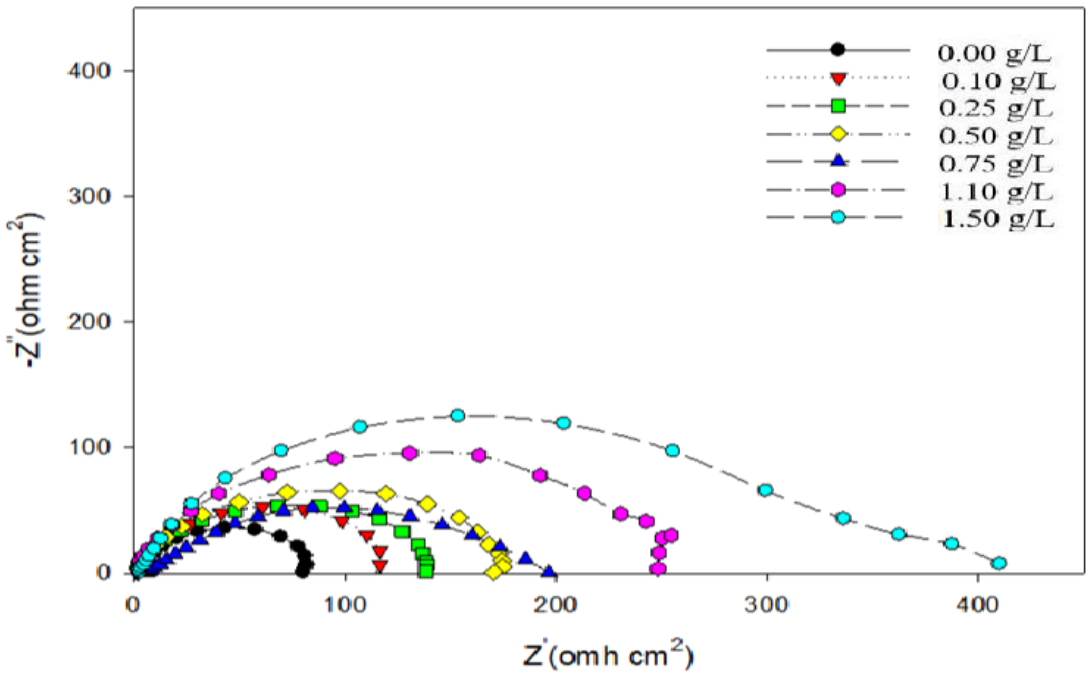

Figure 6. Nyquist plots for mild steel in 1.0 M HCl without and with (0.1-1.5 g/L) concentrations of chitosan-montmorillonite nanocomposite at 30 °C.

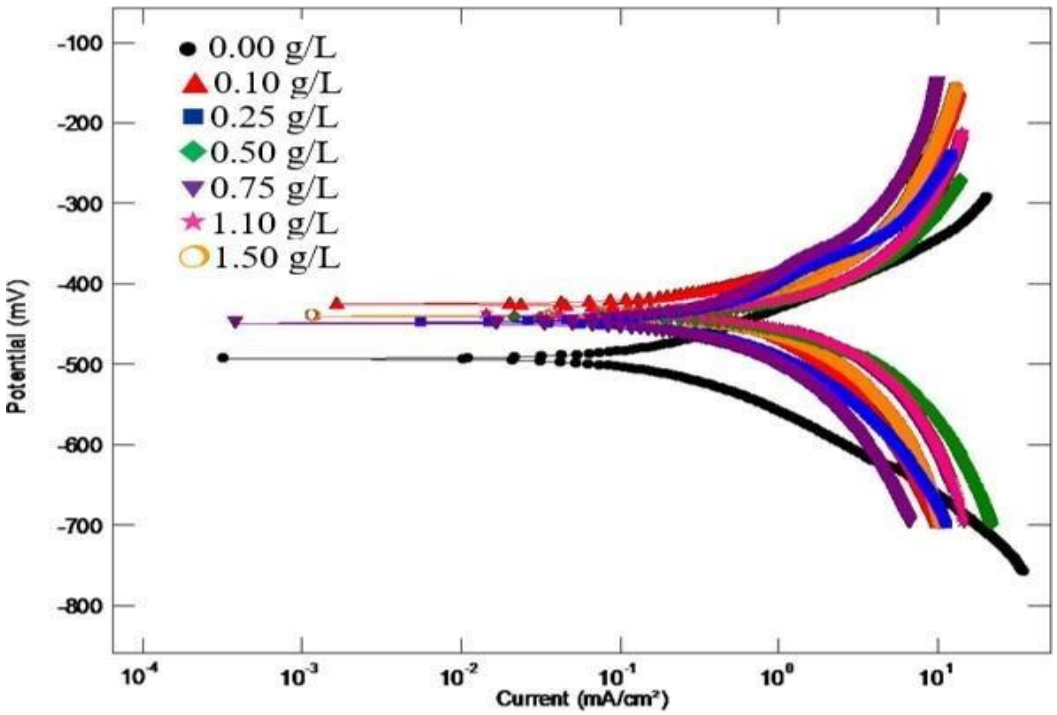

Figure 7. Polarization curves of mild steel immersed in 1.0 M HCl without and with (0.1-1.5 g/L) concentrations of chitosan-montmorillonite nanocomposite at 30 °C.

Table 2. Electrochemical impedance parameter for mild steel specimens in 1.0 M HCl solution with and without different concentrations of chitosan-montmorillonite nanocomposite at 30 °C.

C_{inh} (g/L)	R_s (Ω cm^2)	C_{dl} x10^{-4} (F cm^{-2})	R_{ct} (Ω cm^2)	IE%
0.00	1.53	554.0	72.12	--
0.10	1.50	396.0	118.9	31.08
0.25	0.35	116.4	152.9	44.47
0.50	0.34	83.00	173.2	50.95
0.75	0.83	41.10	202.1	57.86
1.00	0.08	12.70	266.9	68.20
1.50	3.27	1.80	327.9	74.08

Table 3. Polarization parameters of mild steel immersed in 1.0 M HCl without and with different concentrations of chitosan-montmorillonite nanocomposites at 30 °C.

C_{inh} (g/L)	- E_{corr} (mV)	I_{corr} (μA cm^{-2})	β_a (m*V*)	β_c (m*V*)	IE%
0.00	492	1335.9	77	74	--
0.10	424	892.915	82	121	33.16
0.25	445	770.146	88	85	42.35
0.50	440	622.255	36	39	53.42
0.75	449	513.787	91	80	61.54
1.00	440	377.124	32	35	71.77
1.5	439	307.123	43	38	77.01

3.3. Surface Examination Study

3.3.1. Scanning Electron Microscopy (SEM)

Figures (8A-C) depict SEM images of the mild steel “A" before and "B" after immersion in 1.0 M HCl for 3 weeks. SEM images "A" show noncorroded surfaces with scratches due to polishing. The nonhomogeneous nature of mild steel surfaces is evident in images "A". SEM images "B" show damaged surfaces due to localized attack by 1.0 M HCl. "C" shows that in the presence of 0.5 g/L chitosan-montmorillonite nanocomposite; there was a change in the surface morphology due to the presence of the adsorbed layer of chitosan-montmorillonite nanocomposite, which inhibits corrosion.

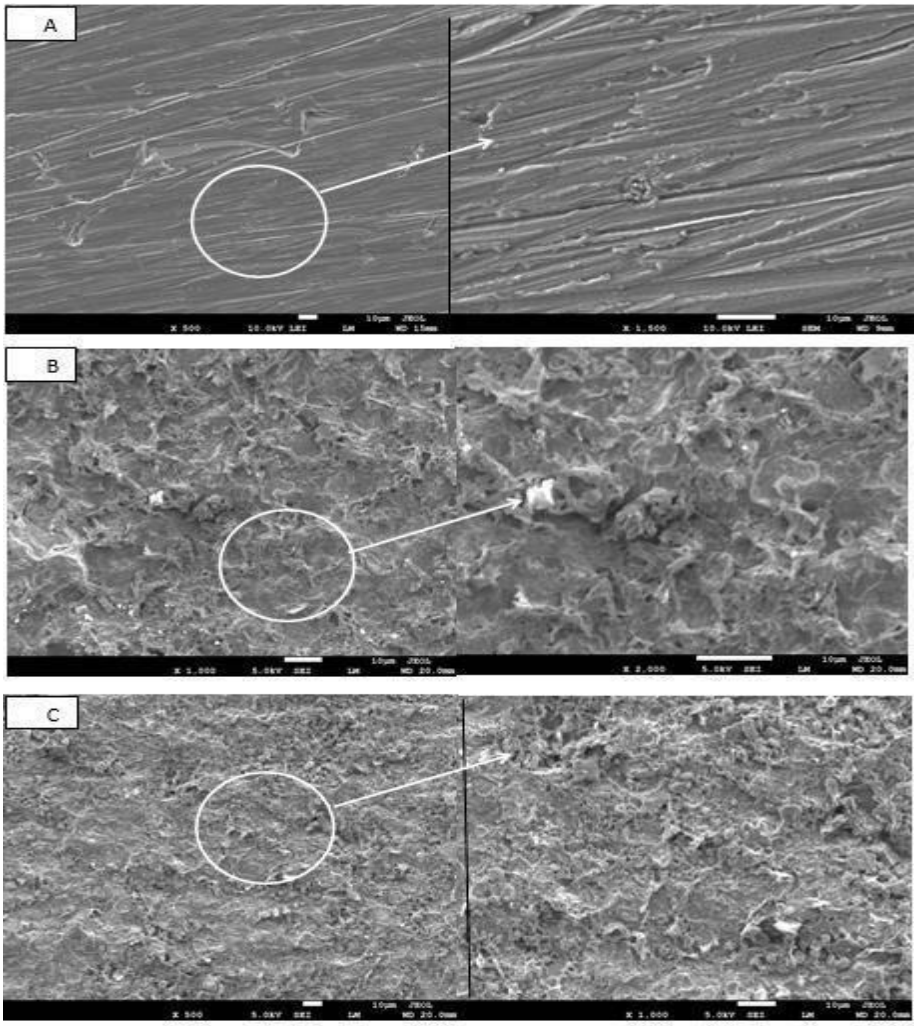

Figure 8. SEM images of mild steel "A" before immersion and "B" after immersion in the 1.0 M HCl and "C" after immersion in 1.0 M HCl +0.5 g/L chitosan-montmorillonite nanocomposite for 3 weeks.

3.3.2. Atomic Force Microscopy (AFM)

The AFM is very important in confirming the efficiency of the 0.5 g/L chitosan-montmorillonite nanocomposite on mild steel corrosion. The images produced by this method are used between several mild steel surfaces [19]. The 3D images for mild steel surface and mild steel immersed in 1.0 M HCl containing 0.5 g/L chitosan-montmorillonite nanocomposite are presented in Figure (9). Roughness data for different mild steel surfaces are given in Table (4). The mild steel surface appears smoother for the roughness data because of the inhibitor adsorption of the mild steel, forming the protective layer [20].

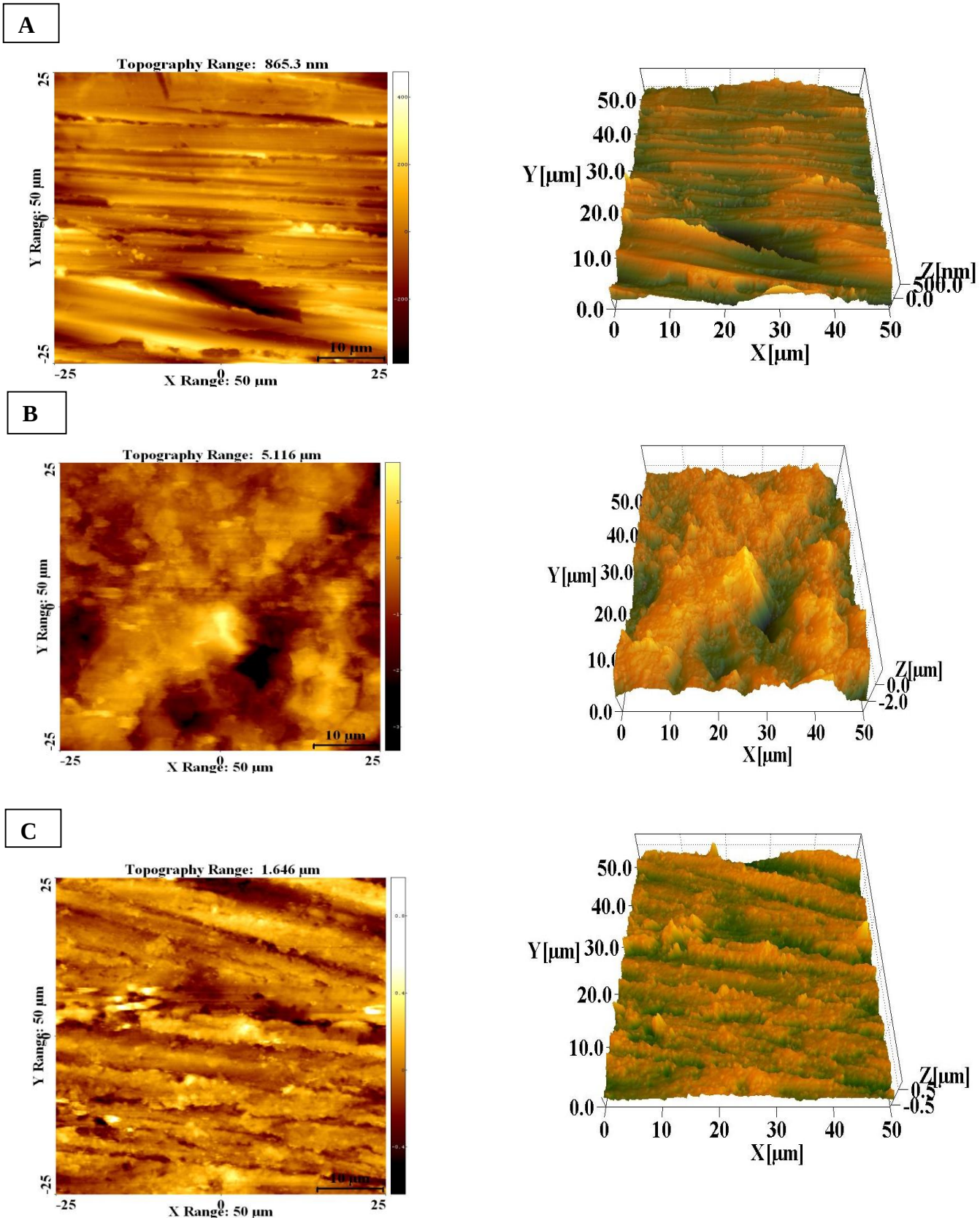

Figure 9. Three-dimensional (3D) AFM micrographs of a mild steel surface (A) before inundation in 1.0 M HCl, (B) after 3 weeks of inundation in 1.0 M HCl and (C) after 3 weeks of inundation in 1.0 M HCl + 0.5 g/L chitosan-montmorillonite nanocomposite at 30 °C.

Table 4. AFM roughness data of mild steel surface immersed for 3 weeks at 30 °C.

Specimen	*Average roughness (Sa) (nm)*
A	70.0447
B	526.119
C	105.485

4. CONCLUSION

Corrosion is the deterioration process of metals, which has a severe impact on our lives in many ways, such as the economy, safety, health, etc. In the present study, we have prepared (chitosan-montmorillonite) nanocomposites as an inhibitor of mild steel in 1.0 M HCl. The composite was characterized by FTIR, NMR, SEM and AFM analyses. The anti-corrosion behavior of the inhibitor was studied by electrochemical measurements, potentiodynamic polarization (PDP) and electrochemical impedance spectroscopy (EIS). The results indicated that nanocomposite inhibits mild steel corrosion in 1.0 M HCl. The PDP results showed that chitosan-montmorillonite nanocomposites act as mixed-type inhibitors.

CONFLICT OF INTERESTS
The authors have declared that there is no conflict of interest.

ACKNOWLEDGMENTS
The authors would like to thank the Department of Chemistry, University of Jeddah, for providing the required facilitie.

References

1. M. Alshabanat, A.Al-Arrash and W. Mekhamer, *J. Nanomater*, 2013 (2013) 650725.
2. K. Barton, Protection against atmospheric corrosion: theories and methods, (1976).
3. K.C. Chang, S. T. Chen, H.F. Lin, C.Y. Lin, H.H. Huang, J.M. Yeh and Y.H. Yu, *Eur. Polym. J*, 44 (2008) 1323.
4. S. Ramasubramaniam, C. Govindarajan, K. Nasreen and P.N. Sudha, *Compos. Interfaces*, 21 (2014) 95.
5. Y. L. Feng, C. Wang, N. Mao, M.T. Wang, L.J. Yu and Z.Q. Wei, *Adv Mater,* 6 (2017) 20.
6. C. Yu, Y. Ke, X. Hu, Y. Zhao, Q. Deng and S. Lu, *Polymers*, 11 (2019) 834.
7. P. Singla, R. Mehta and S.N. Upadhyay, *Green Sustainable Chem*., 2 (2012) 21.

8. C. Kumudinie, Encyclopedia of Materials: Science and Technology (2001) 7574, doi: 10.1016/B0-08-043152-6/01356-5.
9. A.D. M. F. Guimarães, V. S. T. Ciminelli and W. L. Vasconcelos, *Appl. Clay Sci*., 42 (2009) 410.
10. M. Lavorgna, F. Piscitelli, P. Mangiacapra and G.G. Buonocore, *Carbohydr. Polym*. , 82 (2010) 291.
11. R.C.F. Cheung, T.B. Ng, J.H. Wong and W.Y. Chan, *Mar. Drugs*, 13 (2015) 5156.
12. C. Verma, A.M. Kumar, M.A.J. Mazumder and M.A. Quraishi, Chitin-Chitosan: Myriad Functionalities in Science and Technology 143 (2018).
13. J. A. M. Oliveira, R. A. C. de Santana and A. D. O. W. Neto, *Carbohydr. Polym*. , 255 (2021)117382.
14. P. Lertsutthiwong, K. Noomun, S. Khunthon and S. Limpanart, *Prog. Nat. Sci.: Mater. Int*. , 22 (2012) 502.
15. P. K. Dutta, J. Dutta and V.S. Tripathi, *Pak. J. Sci. Ind. Res.Pakistan*, 63(2004) 20.
16. E. Guibal, *Sep. Purif. Technol*. , 38 (2004) 43.
17. K. Muthamma, P. Kumari, M.Lavanya, SA. Rao, *Journal of Bio-and Tribo-Corrosion*, 7 (2021) 1.
18. Y. Rao, D. Sunil, P. Shetty, SA. Rao, *Surf. Eng. Appl. Electrochem*.,55 (2019) 443.
19. M. Cieślik, K. Engvall, J. Pan and A. Kotarba, *Corros. Sci.*, 53 (2011) 296.
20. S. Rajendran, C. Thangavelu and G. Annamalai, *Journal of Chemical and Pharmaceutical Research*, 4 (2012) 4836.